Role of instabilities in the survival of quantum correlations

T. Figueiredo Roque* and J. A. Roversi†

Instituto de Física Gleb Wataghin, Universidade Estadual de Campinas, 13083-859 Campinas, São Paulo, Brazil

(Received 25 March 2013; published 23 September 2013)

This article surveys quantum correlations dynamics, in the Markovian and non-Markovian regimes, in a system of two harmonic oscillators connected by a time-dependent coupling and in contact with a common heat bath. The results show the survival of the quantum correlations, including entanglement, even at very high temperatures, as well as a remarkable relation between entanglement and the instability of the system. The results also show that the indirect interaction of the oscillators via a bath significantly enhances the quantum correlations and that quantum correlations are much more sensitive to the parameters of the oscillators than the temperature of the bath.

DOI: 10.1103/PhysRevA.88.032114 PACS number(s): 03.65.Ud, 42.50.Ar, 03.67.Bg

I. INTRODUCTION

Quantum correlations (QCs) are one of the main features of quantum mechanics. Since the beginnings of quantum theory, QCs have played a major role, sometimes being used to refute the quantum theory, as was done by Einstein, Podolsky, and Rosen in their celebrated paper [1], and sometimes remarkably confirming its previsions, as in Bell's experiments [2]. Since then, the interest in QCs has not been lost. With the advent of quantum computation, for which QCs, especially entanglement, are the main resource, there was a huge interest in qualifying and quantifying these resources. But soon many physicists noted that there was one big problem: decoherence. Decoherence is the mechanism by which a quantum system loses its coherence, and consequently classical behavior emerges. Such a mechanism arises from the interaction of the quantum system with the environment. Therefore, to avoid decoherence would require a very good isolation and cooling of the experimental apparatus, or the decoherence time scale would be so small that we could not observe any quantum effect at all. Thus the real execution of the quantum computer became a very difficult task, and it was necessary to find a way to at least decrease the decoherence effects.

In recent years we have seen several works dealing with the dynamics of QCs in open quantum systems, especially systems of qubits [3–8] or harmonic oscillators [9–14] in contact with the environment. One general conclusion about these works is that temperature has severe effects on the entanglement dynamics, making the observation of highly entangled states in real physical systems a very challenging task. In 2010, however, a paper by Galve *et al*. [15] brought some hope. The authors considered a system of two coupled harmonic oscillators, with a coupling of the form $c(t) = c_0 + c_1 \cos(\omega_D t)$, and in contact with independent heat baths, and they showed the existence of entangled states even at high temperatures. This discovery has very important consequences: from a theoretical point of view, it excludes temperature in the determination of decoherence, and we can find at least one system in which there are high temperatures and still a quantum regime. From an experimental point of view, without the need for a rigorous cooling apparatus, experiments would be easier and less expensive in the laboratory. Finally, the survival of QCs at high temperatures is a huge step toward the realization of a quantum computer.

In this paper, we analyze the Markovian and the non-Markovian dynamics of QCs in a system of two harmonic oscillators connected by a coupling of the form $c(t) = c_0 + c_1 \cos(\omega_D t)$, and in contact with a common heat bath. We show that the survival of QCs in this system, even at high temperatures, is directly related to the instabilities of the system. This unstable behavior is especially pronounced when ω_D is close to twice the oscillator frequency ω_0. One of the consequences of this relation between QCs and instabilities is that the QCs are much more sensitive to variations in the parameters of the system than variations in the temperature of the bath. This result is especially important because in this system, temperature loses importance in the survival of the QCs. The results also suggest that the observation of entangled states, contradicting Bohr's correspondence principle, is possible for any finite temperature and even when the number of quanta of the oscillators is very large. Comparing our results with those of Galve *et al*., we find that the indirect interaction of the oscillators via a bath notoriously contributes to enhancing the QCs.

The paper is organized as follows. In Sec. II, we show the Hamiltonian of our system and how to obtain its temporal evolution. We use a path-integral approach in the Markovian regime and a master equation approach in the non-Markovian regime. In Sec. III, we briefly discuss the quantum correlation measures used in this work. In Sec. IV, we show the temporal evolution of the QCs and their relation with instabilities in both the Markovian and non-Markovian regimes. Section V contains concluding remarks.

II. THE MODEL AND ITS SOLUTION

Our model is described by the following Hamiltonian:

$$H = H_S + H_B + H_I, \tag{1}$$

where

$$H_S = \sum_{i=1,2} \left[\frac{P_i^2}{2m} + \frac{m\omega_0^2}{2} X_i^2 \right] + c(t) X_1 X_2 \tag{2}$$

is the system Hamiltonian, $c(t)/m = c_0 + c_1 \cos(\omega_D t)$ being a time-dependent coupling between oscillators

*tfroque@ifi.unicamp.br
†roversi@ifi.unicamp.br

1 and 2,

$$H_B = \sum_k^{\infty} \left[\frac{p_k^2}{2m_k} + \frac{m_k \omega_k^2}{2} x_k^2 \right] \tag{3}$$

is the bath Hamiltonian, and

$$H_I = \sum_{k=1}^{\infty} \left[-c_k x_k (X_1 + X_2) + \frac{c_k^2}{2m_k \omega_k^2} (X_1 + X_2)^2 \right] \tag{4}$$

is the interaction Hamiltonian. The Hamiltonian (1) is bilinear in the field operators of the system. This implies that if we prepare the system in a Gaussian state, it will remain in a Gaussian state indefinitely [16]. Given that all the information about the QCs in a Gaussian state is contained in the covariance matrix, by now our main interest is in the temporal evolution of the covariance matrix.

Defining the new variables,

$$X_\pm = (X_1 \pm X_2)/\sqrt{2}, \quad P_\pm = (P_1 \pm P_2)/\sqrt{2}, \tag{5}$$

the Hamiltonian can be written in the following way:

$$H = H_+ + H_-, \tag{6}$$

where H_+ is given by

$$H_+ = \frac{P_+^2}{2m} + \frac{m\Omega_+^2(t)}{2} X_+^2 + \sum_{k=1}^{\infty} \left[\frac{p_k^2}{2m_k} + \frac{m_k \omega_k^2}{2} \left(x_k - \frac{\sqrt{2} c_k}{m_k \omega_k^2} X_+ \right)^2 \right], \tag{7}$$

and $\Omega_\pm^2(t) = \omega_0^2 \pm c_0 \pm c_1 \cos(\omega_D t)$. The Hamiltonian (7) describes a parametric oscillator coupled to a bath. The last term in the Hamiltonian (6) is given by

$$H_- = \frac{P_-^2}{2m} + \frac{m\Omega_-^2(t)}{2} X_-^2 \tag{8}$$

and describes a free parametric oscillator. Given that the Hamiltonian is separable, we can treat the two oscillators independently.

A. The classical parametric oscillator

Before studying the quantum parametric oscillators in Hamiltonian (6), we will first consider the classical dissipative parametric oscillator. The equation of motion for such a system is

$$m\ddot{x} + m\gamma\dot{x} + m\omega^2(t)x = 0, \tag{9}$$

where $\omega^2(t) = \omega_0^2 + \epsilon \cos(\omega_D t)$ and γ is the friction coefficient. Defining the adimensional parameters,

$$\tilde{t} = \frac{\omega_D t}{2}, \quad \tilde{\epsilon} = \frac{2c_1}{\omega_D^2}, \quad \tilde{\omega}_0 = \frac{2\omega_0}{\omega_D}, \quad \tilde{\gamma} = \frac{2\gamma}{\omega_D}, \tag{10}$$

we can write the equation of motion in the following way:

$$\ddot{x} + \tilde{\gamma}\dot{x} + \tilde{\omega}^2(\tilde{t})x = 0, \tag{11}$$

where $\tilde{\omega}^2 = \tilde{\omega}_0^2 + 2\tilde{\epsilon}\cos(2\tilde{t})$. As we are going to use only adimensional parameters from now on, we will omit the tilde for convenience. Defining $y = x \exp(-\gamma t/2)$ and substituting

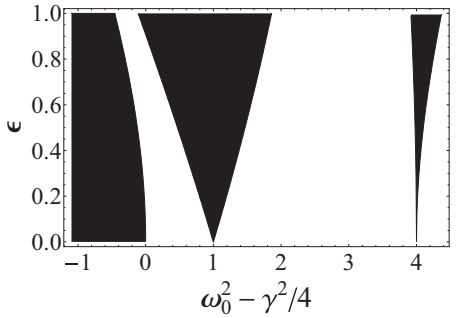

FIG. 1. Stability diagram for the Mathieu equation with a renormalized frequency $\omega_R^2 = \omega_0^2 - \gamma^2/4$. In the black areas we have at least one unstable solution.

in Eq. (11), we get

$$\ddot{y} + \left[\omega_0^2 - \frac{\gamma^2}{4} + 2\epsilon\cos(2t) \right] y = 0. \tag{12}$$

This is a Mathieu equation with a renormalized angular frequency $\omega_R^2 = \omega_0^2 - \gamma^2/4$, and for such an equation we can use the results of the Floquet theory for differential equations [17]. In particular, a possible set of linearly independent solutions for the Mathieu equation are the Floquet solutions, which can be written as

$$\varphi_1(t) = e^{i\nu t} p(t), \quad \varphi_2(t) = \varphi_1(-t), \tag{13}$$

where $p(t)$ is a function of period π and ν is the so called Mathieu characteristic exponent. The characteristic exponent ν governs the stability of the solutions of the Mathieu equation. Whenever $\mathrm{Im}\{\nu\} \neq 0$, there is at least one unstable solution. In Fig. 1, we have the stability diagram for Eq. (12).

For calculation purposes, a more convenient set of solutions satisfy the following initial conditions:

$$\begin{aligned} \phi_1(t_0) &= 0, \quad \dot{\phi}_1(t_0) = 1, \\ \phi_2(t_0) &= 1, \quad \dot{\phi}_2(t_0) = 0. \end{aligned} \tag{14}$$

As the Wronskian of the Mathieu equation is time-independent [18], this is a set of linearly independent solutions. The solutions $\phi_1(t)$ and $\phi_2(t)$ can be obtained via numerical integration of Eq. (12).

B. The quantum parametric oscillator

The quantum parametric oscillator is described by the following adimensional Hamiltonian operator:

$$\tilde{H} = \frac{\tilde{P}^2}{2} + \frac{\tilde{\omega}^2(\tilde{t})}{2} \tilde{X}^2, \tag{15}$$

where $\tilde{P} = \sqrt{\frac{2}{\hbar m \omega_D}}\hat{P}$, $\tilde{X} = \sqrt{\frac{m\omega_D}{2\hbar}}\hat{X}$, and $\tilde{\omega}^2(t) = \tilde{\omega}_0^2 + 2\tilde{\epsilon}\cos(2\tilde{t})$. We can study the dynamics of the quantum parametric oscillator using the Schrödinger equation with the Hamiltonian (15), but as we are interested in the time evolution of the covariance matrix, we can be more pragmatic and use the Ehrenfest theorem to get the following set of coupled differential equations relating the elements of the covariance

matrix:

$$\dot{\sigma}_{xx} = 2\sigma_{xp}, \quad \dot{\sigma}_{xp} = \sigma_{pp} - \omega^2(t)\sigma_{xx}, \\ \dot{\sigma}_{pp} = -2\omega^2(t)\sigma_{xp}. \tag{16}$$

These equations can be decoupled and we get a third-order differential equation for σ_{xx},

$$\dddot{\sigma}_{xx} + 4\omega^2(t)\dot{\sigma}_{xx} + 2\left\{\frac{d}{dt}\omega^2(t)\right\}\sigma_{xx} = 0. \tag{17}$$

Preparing the system in an initial state with variances σ^0_{xx}, σ^0_{xp}, and σ^0_{pp}, the general solution of Eq. (17) can be written in terms of $\phi_1(t)$ and $\phi_2(t)$, defined in Eq. (14), as

$$\sigma_{xx}(t) = \sigma^0_{pp}\phi_1^2(t) + \sigma^0_{xp}\phi_1(t)\phi_2(t) + \sigma^0_{xx}\phi_2^2(t). \tag{18}$$

Thus from Eqs. (16) we get

$$\sigma_{xp}(t) = \sigma^0_{pp}\phi_1(t)\dot{\phi}_1(t) + \sigma^0_{xp}[\phi_1(t)\dot{\phi}_2(t) + \dot{\phi}_1(t)\phi_2(t)] \\ + \sigma^0_{xx}\phi_2(t)\dot{\phi}_2(t) \tag{19}$$

and

$$\sigma_{pp}(t) = \sigma^0_{pp}\dot{\phi}_1^2(t) + \sigma^0_{xp}\dot{\phi}_1(t)\dot{\phi}_2(t) + \sigma^0_{xx}\dot{\phi}_2^2(t). \tag{20}$$

C. The dissipative quantum parametric oscillator

The Hamiltonian operator of the dissipative quantum parametric oscillator is

$$\hat{H} = \frac{\hat{P}^2}{2m} + \frac{m\omega^2(t)}{2}\hat{X}^2 \\ + \sum_{k=1}^{\infty}\left[\frac{\hat{p}_k^2}{2m_k} + \frac{m_k\omega_k^2}{2}\left(\hat{x}_k - \frac{\sqrt{2}c_k}{m_k\omega_k^2}\hat{X}\right)^2\right], \tag{21}$$

where $\omega^2(t) = \omega_0^2 + \epsilon\cos(\omega_D t)$. We will make the hypothesis that for $t \leqslant t_0$, the density operator that describes the total system (oscillator + bath) is factorizable, so we can write it as $\hat{\rho}_{\mathrm{osc}+B} = \hat{\rho}_{\mathrm{osc}} \otimes \hat{\rho}_B$. This implies that the parametric oscillator and the bath starts to interact in $t = t_0$. The bath consists of an infinite number of oscillators, and the spectral density of the bath, defined as

$$I(\omega) = \frac{\pi}{2}\sum_{k=0}^{N}\frac{c_k^2}{m_k\omega_k}\delta(\omega - \omega_k), \tag{22}$$

has all the information about the bath necessary to study the dynamics of the parametric oscillator. Moreover, the spectral density defines a time scale in which memory effects are relevant, leading to two specific regimes: the Markovian regime, where memory effects are negligible, and the non-Markovian, where memory effects must be considered.

1. The Markovian regime

In the Markovian regime, we use the following spectral density:

$$I(\omega) = \begin{cases} m\gamma\omega & \text{if} \quad \omega \leqslant \omega_C, \\ 0 & \text{if} \quad \omega > \omega_C, \end{cases} \tag{23}$$

where ω_C^{-1} gives the time scale in which the memory of the system is important. In the Markovian regime, ω_C must be big enough so that the above-mentioned time scale is much smaller than the time scale considered in this work. For this specific spectral density, we can use the path-integral method of Feynman and Vernon. This method, in principle, can be applied to more general Hamiltonians and to arbitrary spectral densities, but for this spectral density in particular the calculations can be done. For a factorizable initial state, the reduced density operator with respect to the oscillator at time t is given by

$$\rho_{\mathrm{osc}}(x_f, y_f, t) = \int dx_0 dy_0 J(x_f, y_f, t; x_0, y_0, t_0)\rho_{\mathrm{osc}}(x_0, y_0, t_0), \tag{24}$$

where

$$J(x_f, y_f, t|x_0, y_0, t_0) \\ = \int \mathcal{D}x \int \mathcal{D}y \exp\left\{\frac{i}{\hbar}[S(x) - S(y)]\right\}\mathcal{F}(x, y) \tag{25}$$

is called the superpropagator,

$$S(x) = \int_{t_0}^{t}\frac{m}{2}\{\dot{x}^2 - [\omega^2 + \epsilon\cos(\omega_D t)]x^2\}dt \tag{26}$$

is the action of the parametric oscillator, calculated in the classical path linking x_0 to x_f, and

$$\mathcal{F}(x, y) \\ = \exp\left\{-\pi\frac{i}{\hbar}\int_{t_0}^{t}d\tau\int_{t_0}^{\tau}ds[x(\tau) - y(\tau)]I(\omega)\sin\omega(\tau - s)\right. \\ \times [x(s) + y(s)] - \frac{\pi}{\hbar}\int_{t_0}^{t}d\tau\int_{t_0}^{\tau}ds[x(\tau) - y(\tau)] \\ \left.\times I(\omega)\cot\left(\frac{\hbar\omega}{2K_BT}\right)\cos\omega(\tau - s)[x(s) - y(s)]\right\} \tag{27}$$

is called the influence functional of the bath on the system. The double path integral in Eq. (25) is quadratic, so it can be done exactly [19], and the result is

$$J(x_f, y_f, t|x_0, y_0, t_0) \\ = \frac{1}{N(t)}\exp\left\{\frac{i}{\hbar}[S(x_{\mathrm{cl}}) - S(y_{\mathrm{cl}})]\right\}\mathcal{F}(x_{\mathrm{cl}}, y_{\mathrm{cl}}), \tag{28}$$

where $N(t)$ is a normalization factor determined such that $\mathrm{Tr}[\rho(t)] = 1$, and x_{cl} and y_{cl} correspond to the classical paths linking x_i to x_f and y_i to y_f, respectively. Defining $q = x - y$ and $Q = x + y$, these classical paths are determined by the following differential equations:

$$\ddot{Q} + 2\gamma\dot{Q} + \omega^2(t)Q = 0, \quad \ddot{q} - 2\gamma\dot{q} + \omega^2(t)q = 0, \tag{29}$$

which are formally identical to the equation of motion of the classical dissipative parametric oscillator. Thus the solutions of Eqs. (29), with the appropriate boundary conditions at t_0 and t, are

$$Q(s) = Q_0u_1(t, s) + Q_fu_2(t, s), \\ q(s) = q_0v_1(t, s) + q_fv_2(t, s), \tag{30}$$

where

$$u_1(t,s) = f_2(s) - f_1(s)f_2(t)/f_1(t),$$
$$u_2(t,s) = f_1(s)/f_1(t), \quad v_1(t,s) = u_1(t,s)e^{\gamma s}, \tag{31}$$
$$v_2(t,s) = u_2(t,s)e^{\gamma(s-t)},$$

and $f_i(t) = e^{-\gamma t}\phi_1(t)$, with $\phi_i(t)$ defined in Eqs. (14).

Substituting Eq. (30) in Eq. (24), we get the following expression for the superpropagator:

$$J(Q_f,q_f,t;Q_i,q_i,0) = \frac{1}{N(t)}\exp\{i[b_4(t)Q_f q_f - b_3(t)Q_f q_i + b_2(t)Q_i q_f - b_1(t)Q_i q_i]\}\exp\left\{-\left[a_{11}(t)q_i^2 + [a_{12}(t)+a_{21}(t)]q_i q_f + a_{22}(t)q_f^2\right]\right\}, \tag{32}$$

where

$$a_{ij}(t) = \frac{1}{2}\int_{t_0}^{t}\int_{t_0}^{t} v_i(t,\tau)K(\tau - s)v_j(t,s)d\tau\, ds, \tag{33}$$

$$b_1(t) = \dot{u}_1(t,0)/2, \tag{34}$$

$$b_2(t) = \dot{u}_1(t,t)/2, \tag{35}$$

$$b_3(t) = \dot{u}_2(t,0)/2, \tag{36}$$

$$b_4(t) = \dot{u}_2(t,t)/2, \tag{37}$$

and $\dot{u}_1(t,t_0) = \partial u/\partial s|_{s=t_0}$. Now we can obtain the time evolution of the density operator using Eq. (24). A more complete treatment of the quantum parametric oscillator in the Markovian regime can be found in Ref. [20].

2. *The non-Markovian regime*

To study the non-Markovian regime, we could just consider a value of ω_C comparable to the frequencies of the oscillators. However, some steps of the derivation of the path-integral approach were based on the hypothesis of a very high value for ω_C, and the derivation using smaller values for ω_C is not a trivial task. Thus we opted to study the non-Markovian regime using a master equation approach. For this purpose, we will first write the Hamiltonian of the dissipative parametric quantum oscillator, Eq. (21), in terms of the annihilation operators of the system,

$$\hat{a} = \sqrt{\frac{m\omega_0}{2\hbar}}\left(\hat{X} + \frac{i\hat{P}}{m\omega_0}\right),$$
$$\hat{b}_k = \sqrt{\frac{m\omega_k}{2\hbar}}\left(\hat{x}_k + \frac{i\hat{p}_k}{m_k\omega_k}\right), \tag{38}$$

and the result is $\hat{H} = \hat{H}_S + \hat{H}_B + \hat{H}_I$, where

$$\hat{H}_S = \frac{\lambda(t)}{2}\hat{a}^2 + \frac{\lambda^*(t)}{2}\hat{a}^{\dagger 2} + \omega(t)\hat{a}^\dagger\hat{a}, \tag{39}$$

$$\hat{H}_B = \sum_k \omega_k \hat{b}_k^\dagger \hat{b}_k, \tag{40}$$

and

$$\hat{H}_I = \sum_k g_k(\hat{a} + \hat{a}^\dagger)(\hat{b}_k + \hat{b}_k^\dagger). \tag{41}$$

The parameters of the total Hamiltonian are

$$\lambda(t) = \frac{c_0 + c_1\cos(\omega_D t)}{2\omega_0} + \frac{1}{2\omega_0}\int_0^\infty \frac{I(\omega')}{\omega'}d\omega', \tag{42}$$

$$\omega(t) = \omega_0 + \lambda(t), \tag{43}$$

and

$$g_k = \frac{c_k}{2\sqrt{mm_k\omega_k}}. \tag{44}$$

For the above Hamiltonian, Chang and Law proposed a master equation in Ref. [21],

$$\frac{d}{dt}\hat{\rho} = -i[\hat{H}_S(t) + \Delta\hat{H}_S(t),\hat{\rho}] - \gamma_1(t)(\hat{a}^\dagger\hat{a}\hat{\rho} + \hat{\rho}\hat{a}^\dagger\hat{a} - 2\hat{a}\hat{\rho}\hat{a}^\dagger) - \gamma_2(t)(\hat{a}\hat{a}^\dagger\hat{\rho} + \hat{\rho}\hat{a}\hat{a}^\dagger - 2\hat{\rho}\hat{a}^\dagger\hat{a}) - \gamma_3(t)(\hat{a}^2\hat{\rho} + \hat{\rho}\hat{a}^2 - 2\hat{a}\hat{\rho}\hat{a}) - \gamma_3^*(t)(\hat{a}^{\dagger 2}\hat{\rho} + \hat{\rho}\hat{a}^{\dagger 2} - 2\hat{a}^\dagger\hat{\rho}\hat{a}^\dagger), \tag{45}$$

where $\Delta\hat{H}_S = \frac{\Delta\lambda(t)}{2}\hat{a}^2 + \frac{\Delta\lambda^*(t)}{2}\hat{a}^{\dagger 2} + \Delta\omega(t)\hat{a}^\dagger\hat{a}$. Thus the whole problem comes down to calculating the functions $\gamma_i(t)$, $\Delta\lambda(t)$, and $\Delta\omega(t)$. Given the linearity of the Hamiltonian, the operator $\hat{a}$ in the Heisenberg picture can be written as [21]

$$\hat{a}(t) = G(t)\hat{a}(0) + L^*(t)\hat{a}^\dagger(0) + \hat{F}(t), \tag{46}$$

where $\hat{F}(t) = \sum_k[\mu_k(t)\hat{b}_k(0) + \nu_k(t)\hat{b}_k^\dagger(0)]$ and the equations satisfied by $G(t)$, $L(t)$, and $\hat{F}(t)$ are

$$\dot{G}(t) = -i\lambda^*(t)L(t) - i\omega(t)G(t) - \int_0^t ds\, K(t-s)[G(s) + L(s)], \tag{47}$$

$$\dot{L}(t) = i\lambda(t)G(t) + i\omega(t)L(t) + \int_0^t ds\, K(t-s)[G(s) + L(s)], \tag{48}$$

$$\frac{d}{dt}\hat{F}(t) = -i\omega(t)\hat{F}(t) - \int_0^t ds\, K(t-s)[\hat{F}(s) + \hat{F}^\dagger(s)] - i\lambda^*(t)\hat{F}^\dagger(t) - i\sum_k g_k[\hat{b}_k(0)e^{-i\omega_k t} + \hat{b}_k^\dagger(0)e^{i\omega_k t}]. \tag{49}$$

Using a Green's function approach in Eq. (49), it can be written as

$$\hat{F}(t) = -i\int_0^t ds[\Gamma_1(t,s) - \Gamma_2^*(t,s)] \times \sum_k g_k[\hat{b}_k(0)e^{-i\omega_k s} + \hat{b}_k^\dagger(0)e^{i\omega_k s}], \tag{50}$$

where the $\Gamma_i(t,s)$ functions are determined by the following integro-differential equations:

$$\frac{d}{d\tau}\mathbf{\Gamma}(\tau+s,s) + i\mathbf{M}(\tau+s)\mathbf{\Gamma}(\tau+s,s) + \int_0^\tau ds'\mathbf{K}(\tau-s')\mathbf{\Gamma}(s+s',s) = 0, \tag{51}$$

where

$$\mathbf{\Gamma}(t,s) = -i\begin{bmatrix} \Gamma_1(t,s) & \Gamma_2^*(t,s) \\ \Gamma_2(t,s) & \Gamma_1^*(t,s) \end{bmatrix}, \tag{52}$$

$$\mathbf{M}(t) = \begin{bmatrix} \omega(t) & \lambda^*(t) \\ -\lambda(t) & -\omega(t) \end{bmatrix}, \tag{53}$$

and

$$\mathbf{K}(\tau) = -2i\int_0^\infty d\omega I(\omega)\sin(\omega\tau)\begin{bmatrix} 1 & 1 \\ -1 & -1 \end{bmatrix}. \tag{54}$$

Comparing the equations of motion obtained using Eqs. (45) and (46), it can be shown that the functions $\gamma_i(t)$, $\Delta\lambda(t)$, and $\Delta\omega(t)$ can be written in terms of $L(t)$, $G(t)$, and the bath correlation functions $\langle\hat{F}(t)\hat{F}(t)\rangle$, $\langle\hat{F}(t)\hat{F}^\dagger(t)\rangle$, and $\langle\hat{F}^\dagger(t)\hat{F}(t)\rangle$. The expressions for $\gamma_i(t)$, $\Delta\lambda(t)$, and $\Delta\omega(t)$ are too cumbersome and will not be shown here, but they can be found in Ref. [21]. Therefore, as is common in non-Markovian dynamics, we have a set of integro-differential equations to solve. We have solved these equations numerically, using the algorithm presented in Ref. [22]. Due to the numerical method used, we have used, for convenience, the following spectral density with smooth regularization:

$$I(\omega) = m\gamma\omega\exp\left\{-\left(\frac{\omega}{\omega_C}\right)^2\right\}. \tag{55}$$

The reader may be asking why we do not just use the master equation approach to study our system in the Markovian and non-Markovian regimes, as the former could be obtained just taking the limit $\omega_C \to \infty$. Indeed we can do that, but the calculations involved in the path-integral approach are much more efficient than the calculations involved in the master equation approach. Thus calculating the Markovian behavior using the former method, besides saving computation time, gives us a way to compare the obtained results via completely different methods.

III. QCs IN GAUSSIAN STATES

Gaussian states are completely determined by their first and second moments. As the first moments can be made zero by local unitary transformations, the QCs in a Gaussian state depend only on its second moments, i.e., on the covariance matrix σ. For a bipartite system, the covariance matrix is defined as $\sigma_{i,j} = \langle(R_iR_j + R_jR_i)\rangle/2 + \langle R_i\rangle\langle R_j\rangle$, and it has the following generic form:

$$\sigma = \begin{bmatrix} \alpha & \gamma^T \\ \gamma & \beta \end{bmatrix}, \tag{56}$$

where $\mathbf{R} = \{X_1, P_1, X_2, P_2\}$ and each greek letter is a 2×2 matrix. By virtue of the constraints imposed by the symmetry property and the uncertainty principle, the QCs can be written in terms of four quantities [23],

$$A = \det[\alpha], \quad C = \det[\gamma], \quad B = \det[\beta], \quad D = \det[\sigma], \tag{57}$$

which are called symplectic invariants. As the positive partial transposition (PPT) criterion is a necessary and sufficient condition for the separability in Gaussian states [24], the entanglement can be measured via logarithmic negativity (En) [25],

$$En = \begin{cases} 0 & \text{if} \quad \tilde{\nu}_- \geqslant 1/2, \\ \log(2\tilde{\nu}_-) & \text{if} \quad \tilde{\nu}_- < 1/2, \end{cases} \tag{58}$$

where $2\nu_\pm^2 = \tilde{\Delta} \pm \sqrt{\tilde{\Delta}^2 - 4D}$ and $\tilde{\Delta} = A + B - 2C$.

It would be interesting also to calculate the quantum discord, but there is no analytic expression available for Gaussian states. However, there is an approximation to the quantum discord in Gaussian states: the Gaussian discord (GD) [26], which is given by

$$\mathrm{GD}(A:B) = f(\sqrt{B}) - f(\nu_+) - f(\nu_-) + I(A,B,C,D), \tag{59}$$

where $f(x) = (x+\frac{1}{2})\ln(x+\frac{1}{2}) - (x-\frac{1}{2})\ln(x-\frac{1}{2})$ and

$$I(A,B,C,D) = \begin{cases} \frac{2C^2+(B-1)(D-A)+2|C|\sqrt{C^2+(B-1)(D-A)}}{(B-1)^2} & \text{if} \quad (D-AB)^2 \leqslant (1+B)C^2(A+D); \\ \frac{AB-C^2+D-\sqrt{C^4+(D-AB)^2-2C^2(AB+D)}}{2B} & \text{otherwise.} \end{cases} \tag{60}$$

IV. RESULTS

In the results presented here, we have used the adimensional time $\tau = \omega_0 t$, and the parameters of the system were put in terms of ω_0 and $T_0 = \hbar\omega_0/K_B$. We have considered that both oscillators are initially in the coherent state $|\alpha\rangle$, where $\alpha = (1+i)/\sqrt{2}$, and we have used $\gamma = 0.005\omega_0/\sqrt{2}$. In the Markovian regime, $\omega_C = 200\omega_0$. We have also defined two relevant parameters to the study of the QCs: τ_R, which is the value of τ after which the system is always in an entangled state, and r, which is the average velocity of the entanglement growth.

In Fig. 2, we have the time evolution of the En and the GD. The results show that even at very high temperatures the system remains entangled for long times (by which we mean $\tau \gg 1$). Let us take a closer look at Fig. 2(a). After some time, the En curve is approximately linear in τ (if we disregard the small oscillations). This behavior repeats itself whenever we have small values for c_0 and c_1, and if we fit this line, we can estimate r as being its angular coefficient and τ_R as being the value of τ at which the line crosses the τ axis. In general, these estimates for τ_R and r are reliable only for small values of c_0 and c_1. With respect to the GD, we can note that it initially shows a fast increase. For some $\tau < \tau_R$, the GD starts to decrease, and only after the entanglement birth ($\tau \approx \tau_R$) does it increase again. The maximum value reached by the GD in this first region ($\tau < \tau_R$) is directly proportional to the value of τ_R. We have observed this behavior in all our simulations. We do not have a conclusive explanation for this

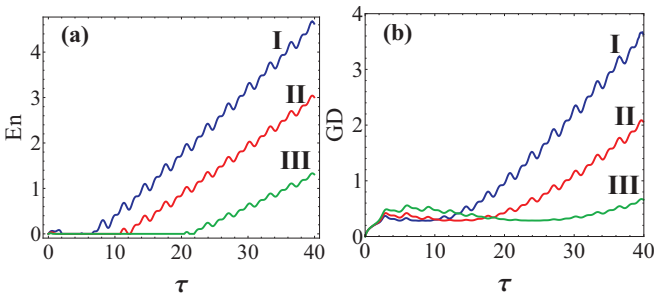

FIG. 2. (Color online) QCs against τ in the Markovian regime for $c_1 = 0.4\omega_0^2$ (I, blue curve), $c_1 = 0.3\omega_0^2$ (II, red curve), and $c_1 = 0.2\omega_0^2$ (III, green curve). In all the curves, $T = 100T_0$, $c_0 = 0$, and $\omega_D = 2\omega_0$.

counterintuitive behavior. It is important to observe that the GD is always different from zero.

In Figs. 3 and 4, we show a more quantitative treatment of τ_R and r. In Fig. 3(a), we have plotted τ_R against T, and the data show that τ_R is a monotonically increasing function of T. The data also suggest a logarithmic dependence in T. We have done a linear fit in $\ln(T)$ and the result is in the same figure. In Fig. 3(b), we have plotted τ_R against c_1, and the data show that τ_R is a monotonically decreasing function of c_1. When c_1 tends to infinity, τ_R tends to zero, and when c_1 tends to zero, τ_R tends to infinity. This suggests a linear fit in some power of c_1^{-1}. We have done a linear fit in c_1^{-1}, and the result is in the same figure. In Fig. 4(a), we have plotted r versus T. Here we cannot see any dependence of r on T. This is confirmed by the inaccurate and very small value obtained for the angular coefficient in the linear fit done in T. However, in Fig. 4(b) there is clearly a linear dependence of r in c_1. The accurate linear fit that was done confirms this observation. It is interesting to note that in all these figures, we could observe entanglement at very high temperatures. These dependences of τ_R and r in T and c_1 were observed in all simulations done, even with very high values of T. There is no guarantee that these relations are valid for much bigger values of τ. However, at least for the values of τ simulated, we note important consequences. The first is that the entanglement dynamics is more sensitive to variations in the coupling parameter c_1 than in the temperature T. Furthermore, it is important to observe that these dependences imply that even for very large values of

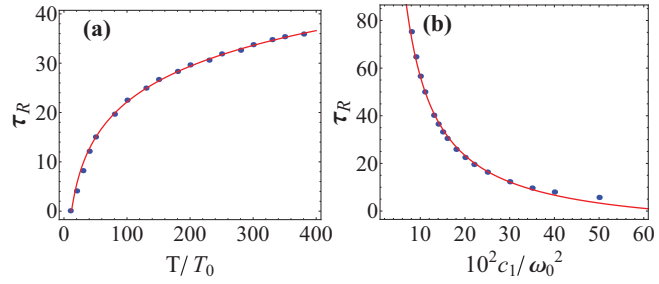

FIG. 3. (Color online) (a) τ_R against T at $c_1 = 0.2\omega_0^2$, $c_0 = 0$, and $\omega_D = 2\omega_0$. The fitted curve is $\tau_R = (10.4 \pm 0.2)\ln(T/T_0) - (25.9 \pm 0.8)$. (b) τ_R against c_1 at $T = 100T_0$, $c_0 = 0$, and $\omega_D = 2\omega_0$. The fitted curve is $\tau_R = (6.6 \pm 0.1)(c_1/\omega_0^2)^{-1} - (9.9 \pm 0.7)$. Both graphs were obtained in the Markovian regime.

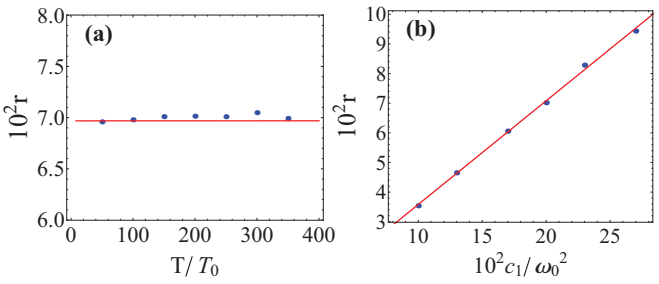

FIG. 4. (Color online) (a) r against T for $c_1 = 0.2\omega_0^2$ and $\omega_D = 2\omega_0$. The fitted curve is $r = (1.7 \pm 0.9) \times 10^{-6} T/T_0 + (6.97 \pm 0.02) \times 10^{-2}$. (b) r against c_1 for $T = 100T_0$ and $\omega_D = 2\omega_0$. The fitted curve is $r = (0.350 \pm 0.007)c_1/\omega_0^2 + (8 \pm 4) \times 10^{-4}$. Both graphs were obtained in the Markovian regime.

T, there is still a value $\tau = \tau_R$ after which the system is in an entangled state, and the "entanglement growth parameter" r is not modified if we compare it with the case of a much smaller heat bath temperature.

When we look at the QCs dependence in ω_D, an interesting behavior is observed. The QCs are extremely sensitive to variations in ω_D, and this sensitivity is related to the instability of the system. In Fig. 5(a), we have the imaginary part of ν, the Mathieu characteristic exponent, against ω_D for both modes (that is, the "+" and the "−" mode), while in Fig. 5(b) we have plotted En against τ for different values of ω_D. Our calculations have shown that only for $\omega_D = 1.96\omega_0$ and $\omega_D = 2\omega_0$, which are values that lead to unstable behavior (because $\mathrm{Im}\{\nu\} \neq 0$), we observe entanglement for long times. This behavior has repeated itself in all calculations done. It is important to note that whenever we have $c_0 = 0$ and $\gamma \ll \omega_0$, we have this kind of graph for $\mathrm{Im}\{\nu\}$, the only difference being that for smaller values of c_1, the peaks observed become smaller and narrower around their centers. This implies that, given $c_0 = 0$ and $\gamma \ll \omega_0$, whenever $\omega_D = 2\omega_0$, the system will be in an unstable dynamics. This tells us that in all the other graphs presented before, the system was in an unstable dynamics, and that is why we could observe entanglement. But until now, we have not considered the effect of adding a static coupling ($c_0 \neq 0$) in this system. In Fig. 6(a), we have the imaginary part of ν against ω_D, but now with $c_0 = 0.05\omega_0^2$. We observe that the intervals of instability of the "+" and "−"

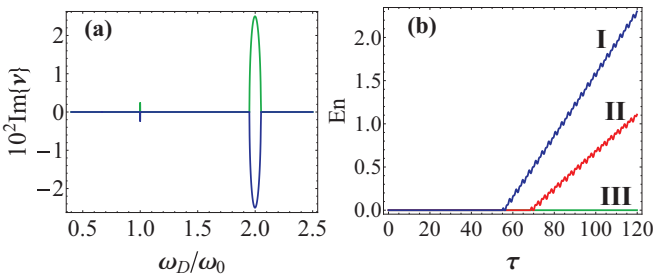

FIG. 5. (Color online) (a) $\mathrm{Im}\{\nu\}$ against ω_D for $c_0 = 0$ and $c_1 = 0.1\omega_0^2$ for the "−" mode (I, green curve) and the "+" mode (II, blue curve). (b) QCs against τ in the Markovian regime for $\omega_D = 1.94\omega_0$ (III, green curve), $\omega_D = 1.96\omega_0$ (II, red curve), and $\omega_D = 2\omega_0$ (I, blue curve). All the curves were obtained with $T = 100T_0$, $c_0 = 0$, and $c_1 = 0.1\omega_0^2$.

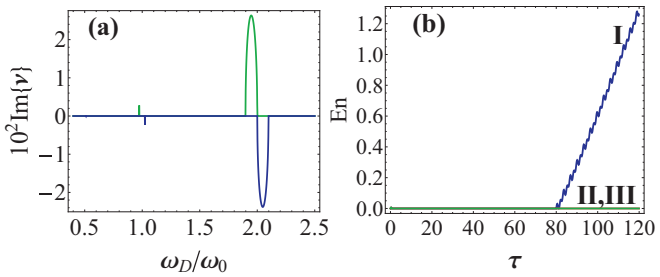

FIG. 6. (Color online) (a) Im{ν} against ω_D for the "−" mode (I, green curve) and the "+" mode (II, blue curve). (b) QCs against τ in the Markovian regime for $\omega_D = 1.96\omega_0$ (I, blue curve), $\omega_D = 2.04\omega_0$ (II, red curve), and $\omega_D = 1.8\omega_0$ (III, green curve). In all the curves, $T = 100T_0$, $c_0 = 0.05\omega_0^2$, and $c_1 = 0.1\omega_0^2$.

modes are not the same anymore. As c_0 appears with a different sign in the equations of each of the "+" and "−" modes, it causes a left shift in the green curve and a right shift in the blue curve. As long as the instability regions of the two modes are no longer the same, we can study the entanglement dynamics when only one mode shows unstable behavior. In Fig. 6(b) we have En for different values of ω_D, and the results show that only for $\omega_D = 1.96\omega_0$, which is the value that leads to an unstable behavior in the "−" mode, we observe entanglement for long times.

In the general case in which we have arbitrary values for the three coupling parameters, c_0, c_1, and ω_D, all the simulations showed that we only observe entanglement at high temperatures and for long times when the "−" mode has an unstable dynamics. This relation between the QCs and instabilities explains why the QCs seem to be so much more sensitive to the oscillator parameters than the bath parameters. In fact, ν does not depend on T (ν depends on γ, but $\gamma \ll \omega_0$ in realistic situations, so it does not make any difference), therefore we expect the system to be less sensitive to variations in T.

Until now, all the results presented were in the Markovian regime. In Fig. 7, we have the QCs in the non-Markovian and in the Markovian regimes. Comparing the two regimes, we can see that for smaller values of ω_C, the En have reached bigger values. Moreover, for $\omega_C = 5\omega_0$ we practically have the same results of the Markovian regime. We can explain the relation between En and ω_C if we take a look at the density spectrum for two different values of ω_C. For smallers values,

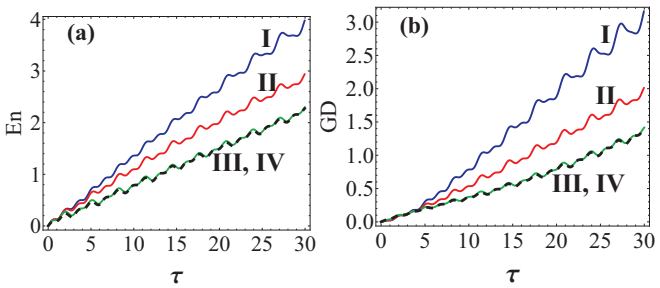

FIG. 7. (Color online) QCs against τ in the non-Markovian regime for $\omega_C = 0.5\omega_0$ (I, blue curve), $\omega_C = 1.0\omega_0$ (II, red curve), and $\omega_C = 5.0\omega_0$ (III, green curve). The dashed curve (IV) refers to the Markovian regime. In all the curves, $T = 10T_0$, $c_1 = 0.2\omega_0^2$, $c_0 = 0$, and $\omega_D = 2\omega_0$.

the system behaves as if it were more weakly coupled to the bath, so we can expect that decoherence effects would be more discreet. The relation between stability and QCs observed in the Markovian regime remains valid in the non-Markovian regime; the instability of the "−" mode is the necessary and sufficient condition to observe entanglement at long times and high temperatures. In the non-Markovian regime, the linear behavior of the En curve is not verified, so we cannot use the definitions of τ_R and r used before. However, redefining τ_R as the value of τ in which was observed the last revival of the entanglement, we can find the same dependence on $\ln(T)$ and c_1^{-1} that was found in the Markovian regime.

The dynamics of the entanglement of two (time independently) coupled harmonic oscillators in contact with a common heat bath in the Markovian [14] and in the non-Markovian [12,13] regimes has already been considered. (Actually, in Ref. [12], the authors have done the rotating-wave approximation in the interaction Hamiltonian. In our work, we do not make this approximation.) In Ref. [14], the authors show that a steady state of entanglement for such a system depends crucially on the initial state of the oscillators, while in Refs. [12,13], An *et al.* show that by taking a two-mode squeezed state for an initial state, it is possible to reach an entangled steady state (with an environment that is assumed to be at zero temperature). Our results show that if $c_1 = 0$ and $c_0 \neq 0$, as the system is going to be stable (at least for $c_0 < \omega_0^2$), we will not measure any entanglement for a long time. Given that we consider a high-temperature environment and we use coherent states as initial states for the oscillators, there is no inconsistency between our results and the results in Ref. [12]. In Ref. [13], however, the authors find smaller measures for the entanglement in the non-Markovian regime if compared with the Markovian regime. Our results go in the opposite way, and we believe that the choice of the initial state is crucial to this behavior.

The results obtained so far relate entanglement to instabilities, which in the case of parametric oscillators translates into oscillations whose amplitudes are proportional to $\exp(\mathrm{Im}\{\nu\}t)$. Thus one would expect that the system is taken to states in which the energy freely increases with time. Figure 8 shows the mean energy of the system in units of $\hbar\omega_0$ in two situations in which entanglement for long times has been observed, i.e.,

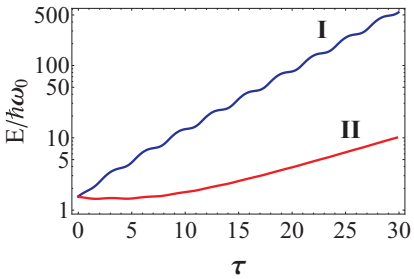

FIG. 8. (Color online) Mean energy of the system in units of $\hbar\omega_0$. The blue (I) curve refers to the case in which $c_1 = 0.4\omega_0^2$, $c_0 = 0$, $\omega_D = 2\omega_0$, and $T = 100T_0$ in the Markovian regime (which is the same situation found in Fig. 2 for the blue curve), and the red (II) curve refers to $c_1 = 0.2\omega_0^2$, $c_0 = 0$, $\omega_D = 2\omega_0$, $\omega_C = 0.5\omega_0$, and $T = 10T_0$ in the non-Markovian regime (which is the same situation found in Fig. 7 for the blue curve).

the blue curve in Fig. 2 and the blue curve in Fig. 7. We can see that the mean energy increases monotonically with time for both curves. Therefore, the system is taken to a highly energetic entangled state. This is especially important because it confirms that the quantum behavior is not exclusive to systems described by very small parameters, as is claimed in the correspondence principle. The results suggest that even if the mean energy of the system is composed by a macroscopic number of excitations, the system still can be found in an entangled state.

Another point that deserves attention is that we could not observe a steady state of entanglement for which $En \neq 0$ in any of our simulations. Indeed, nothing prevents the system from reaching a steady state for much bigger values of τ than we could simulate. However, it would not surprise us if the system never reached a steady state. We must remember that the classical analog of our system can present instability in the Lyapunov sense. So there is no guarantee that our system will reach a steady state. And as we deal with a continuous variable entanglement, there is no superior bound for En; it can keep growing indefinitely.

V. CONCLUSIONS

In this work, we have considered two harmonic oscillators connected by a coupling of the type $c(t) = c_0 + c_1 \cos(\omega_D t)$ and in contact with a common heat bath. We have studied this system in both the Markovian and non-Markovian regimes. In general, in the times simulated, we could obtain high values for the En and GD, even at very high temperatures. The values reached by the En were significatively bigger than the values obtained in Ref. [15], where the oscillators were coupled to independent heat baths. This suggests that the indirect interaction of the oscillators via the heat bath, despite not being sufficient to entangle the oscillators by itself, plays an important role in the dynamics of the QCs. In the times simulated, no entangled steady state was observed.

The results show that, in the times simulated, the instabilities of the system have a crucial and close relationship with the dynamics of the QCs. We have observed that the instability in the "−" mode is a necessary and sufficient condition for the existence of entangled states at high temperatures and for long times. This implies that, for the kind of coupling considered here, the ratio ω_D/ω_0 is extremely important, very small variations of this ratio can change the system from a stable to an unstable dynamics, or vice versa. The case $\omega_D/\omega_0 = 2$ is especially important because whenever $c_0 = 0$ (and $\gamma \ll \omega_0$), this ratio leads to unstable dynamics. In particular, for small values of c_1 and c_0, we could find two parameters that characterize the entanglement: the revival time τ_R and the entanglement growth velocity r. The results show that τ_R is linear in $\ln(T)$ and in c_1^{-1}, while r is linear in c_1 and has no dependence in T. The dependence of these parameters in T is especially important because it implies the possibility of observing entangled states at arbitrarily high temperature. In general, these results show that the oscillator parameters are much more relevant to the QCs dynamics than the bath parameters. With respect to the GD, it is more robust than the En in the sense that it always has a nonzero measure for $\tau > 0$ in all simulations done.

In the non-Markovian regime, we could obtain higher values for the QCs than those obtained in the Markovian regime. This increase is explained by the fact that the smaller the ω_C value is, the more weakly the system is coupled to the environment. Consequently, decoherence effects are less pronounced. The relation between QCs and the instability of the "−" mode observed in the Markovian regime is still valid in the non-Markovian regime.

Lastly, we have shown that the system reaches highly energetic entangled states, suggesting that the observation of entanglement in states with a macroscopic number of excitations is in principle possible.

ACKNOWLEDGMENTS

This work was supported by the Conselho Nacional de Desenvolvimento Científico e Tecnológico (CNPq) and by the Fundação de Amparo à Pesquisa do Estado de São Paulo (FAPESP) (project No. 2011/04521-0).

[1] A. Einstein, B. Podolsky, and N. Rosen, Phys. Rev. **47**, 777 (1935).
[2] J. S. Bell, Physics **1**, 195 (1964).
[3] M. B. Plenio, S. F. Huelga, A. Beige, and P. L. Knight, Phys. Rev. A **59**, 2468 (1999).
[4] M. S. Kim, J. Lee, D. Ahn, and P. L. Knight, Phys. Rev. A **65**, 040101 (2002).
[5] T. Yu and J. H. Eberly, Phys. Rev. Lett. **93**, 140404 (2004).
[6] D. Braun, Phys. Rev. Lett. **89**, 277901 (2002).
[7] M. Paternostro, W. Son, and M. S. Kim, Phys. Rev. Lett. **92**, 197901 (2004).
[8] Z. Ficek and R. Tanas, Phys. Rev. A **74**, 024304 (2006).
[9] D. Vitali, S. Mancini, and P. Tombesi, J. Phys. A **40**, 8055 (2007).
[10] M. J. Hartmann and M. B. Plenio, Phys. Rev. Lett. **101**, 200503 (2008).
[11] M. B. Plenio and S. F. Huelga, Phys. Rev. Lett. **88**, 197901 (2002).
[12] J.-H. An and W.-M. Zhang, Phys. Rev. A **76**, 042127 (2007).
[13] J.-H. An, M. Feng, and W.-M. Zhang, Quant. Inf. Comput. **9**, 0317 (2009).
[14] C-H. Chou, T. Yu, and B. L. Hu, Phys. Rev. E **77**, 011112 (2008).
[15] F. Galve, L. A. Pachon, and D. Zueco, Phys. Rev. Lett. **105**, 180501 (2010).
[16] B. L. Schumaker, Phys. Rep. **135**, 317 (1986).
[17] Z. X. Wang and D. R. Guo, *Special Functions* (World Scientific, Singapore, 1989).
[18] N. W. McLachlan, *Theory and Application of Mathieu Functions* (Dover, New York, 1964).
[19] R. P. Feynman and A. R. Hibbs, *Quantum Mechanics and Path Integrals* (McGraw-Hill, New York, 1965).
[20] C. Zerbe and P. Hanggi, Phys. Rev. E **52**, 1533 (1995).

[21] K. W. Chang and C. K. Law, Phys. Rev. A **81**, 052105 (2010).
[22] J. Wilkie and Y. M. Wong, J. Phys. A **41**, 33 (2008).
[23] S. Olivares, Eur. Phys. J. Spec. Top. **203**, 3 (2012).
[24] R. Simon, Phys. Rev. Lett. **84**, 2726 (2000).
[25] G. Vidal and R. F. Werner, Phys. Rev. A **65**, 032314 (2002).
[26] G. Adesso and A. Datta, Phys. Rev. Lett. **105**, 030501 (2010).